Article

Static Reservoir Simulations and Seismic Attributes Application to Image the Miocene Deep-Water Reservoirs in Southeast Asia

Muhammad Tayyab Naseer [1,2,*], Raja Hammad Khalid [2], Shazia Naseem [2], Wei Li [3,4], George Kontakiotis [5,*], Ahmed E. Radwan [6], Hammad Tariq Janjuhah [7] and Assimina Antonarakou [5]

1   Center for Earthquake Studies, National Center for Physics, Quaid-I-Azam University Campus, Islamabad 44000, Pakistan
2   Department of Earth Sciences, Quaid-I-Azam University, Islamabad 44000, Pakistan; hammad.bs.gp@gmail.com (R.H.K.); drshazianaseem7@gmail.com (S.N.)
3   State Key Laboratory of Petroleum Resources and Prospecting, China University of Petroleum (Beijing), Beijing 102249, China; wei_li@cup.edu.cn
4   College of Geosciences, China University of Petroleum (Beijing), Beijing 102249, China
5   Department of Historical Geology-Paleontology, Faculty of Geology and Geoenvironment, School of Earth Sciences, National and Kapodistrian University of Athens, Panepistimiopolis, Zografou, 15784 Athens, Greece; aantonar@geol.uoa.gr
6   Faculty of Geography and Geology, Institute of Geological Sciences, Jagiellonian University, Gronostajowa 3a, 30-387 Kraków, Poland; radwanae@yahoo.com
7   Department of Geology, Shaheed Benazir Bhutto University, Sheringal 18050, Pakistan; ham-mad@sbbu.edu.pk
*   Correspondence: mtayyab.naseer1@gmail.com (M.T.N.); gkontak@geol.uoa.gr (G.K.)

Abstract: Globally, deep-water reservoir systems are comprised of a variety of traps. Lateral and downdip trapping features include sand pinch-outs, truncation against salt or shale diapirs, and monoclinal dip or faulting with any combination of trapping designs; the potential for massive hydrocarbon accumulations exists, representing significant exploration prospects across the planet. However, deep-water turbidites and submarine fans are two different types of traps, which are developed along the upslope and the basin floor fans. Among these two traps, the basin floor fans are the most prolific traps as they are not influenced by sea-level rise, which distorts the seismic signals, and hence provides ambiguous seismic signatures to predict them as hydrocarbon-bearing zones for future explorations. Therefore, the deep-water channel-levee sand systems and basin floor fans sandstone define economically viable stratigraphic plays. The subsurface variability is significant, and hence, characterizing the thick (porous) channelized-basin floor fans reservoir is a challenge for the exploitation of hydrocarbons. This study aims to develop seismic-based attributes and wedge modeling tools to accurately resolve and characterize the porous and gas-bearing reservoirs using high-resolution seismic-based profiles, in SW Pakistan. The reflection strength slices better delineate the geomorphology of sand-filled channelized-basin floor fans as compared to the instant frequency magnitudes. This stratigraphic prospect has an area of 1180 km^2. The sweetness magnitudes predict the thickness of channelized-basin floor fans as 33 m, faults, and porous lithofacies that complete a vital petroleum system. The wedge modeling also acts as a direct hydrocarbon indicator (DHI) and, hence, should be incorporated into conventional stratigraphic exploration schemes for de-risking stratigraphic prospects. The wedge model resolves a 26-m thick hydrocarbon-bearing channelized-basin floor fans lens with a lateral distribution of ~64 km. Therefore, this wedge model provides ~75% correlation of the thickness of the LSL as measured by sweetness magnitudes. The thickness of shale that serves as the top seal is 930 m, the lateral mud-filled canyons are 1190 m, and the thick bottom seal is ~10 m, which provides evidence for the presence of a vibrant petroleum play. Hence, their reveals bright opportunities to exploit the economically vibrant stratigraphic scheme inside the OIB and other similar global depositional systems.

1. Introduction

Deep-marine systems are one of the hot topics in the stratigraphic exploration of hydrocarbon-bearing plays [1–4]. Sub-marines have an explicit focus on oil and gas practices, and as a result, they are active organic complex pools in deep-offshore environments. The relevant geometrical aspects, as well as associated interior lithology and thickness, in addition to porosity, contribute significantly to promote characterization within pool complexity and non-uniformity. The qualitative studies on these gigantic pools have proven that they have higher quality, i.e., the highest porosity, permeability, and net-to-gross (N/G), of deep-marine sand fills, which remain among the finest of the numerous clastic surroundings that embrace basins. Moreover, under promising circumstances, deep-marine coarse-grained sand-filled pools might remain ponded despite being steeply hooked on identically thick, sand-rich interims. The characterization of these reservoirs by numerous wells can be extraordinarily expensive. However, it can be inferred from the basin description that the channel-levee system and basin floor fans are compartmentalized inside the highly variable mud-filled lithology that makes an excellent stratigraphic trap [1,3,5]. These inferences can be successfully achieved by using seismic-based attributes and wedge modeling techniques. For instance, fuzzy logic can enhance the characterization of diversified lateral systems and their fluid dynamics, since the fluids are diverse and inconsistent due to the geometrical configurations of the reservoir traps. Therefore, the application of these tools may help to visualize in a more quantitative-based attribute analysis of the energy resources [6–9].

Previously, in the offshore Indus Basin (OIB), the reservoir characterization was based on structural and lithological aspects [10,11]. However, until now, there has been no evidence of stratigraphic exploitation of oil and gas reservoirs. In comparison to the techniques stated above, the current study takes a novel strategy and uses seismic-based characteristics and wedge modeling tools to focus on the reservoir stratigraphy of the channel-levee system and basin floor fan pools inside the OIB. These properties have demonstrated their effectiveness in the delineation of bright clastic and carbonate stratigraphic plays, combined with wedge modeling [12–17]. These properties can be broadly divided into two categories: geometrical and physical [16,18–20]. Reservoir architecture is the only thing the geometrical features can define. However, physical characteristics determine the real lithology, the reservoir geometry (faults and fractures) that separates the active lithofluids including oil and gas, and consequently the entire stratigraphic play [13,15,16,19–21]. Thus, the methods used for characterizing these channelized levee structures besides basin floor fan stratigraphic systems are physical properties, particularly amplitude-based ones such as seismic-based amplitude, immediate frequency, envelope strength, and sweetness magnitudes. The current study's objective is to use high-resolution seismic-based profiles to assess the channelized-basin floor fan reservoirs in the OIB, SW Pakistan, in terms of lithology, thickness, and possible porosity impacts.

2. Geological Backgrounds and Petroleum Traits

The Indus River is approximately 2900 km long and moves approximately 1200 km before cutting through the grasslands and setting off to the highlands within the entire drainage region of 966,000 km^2. This watercourse obligates the development of the OIB, which stands as the subsequent biggest solitary system around the globe, the Bengal deltaic system (Figure 1a).

This system has been a principal intended objective of exploration recently; at the present time, the main assortment that includes carbonates and clastic groups is revealed offshore universally (Figure 1a). A variety of boreholes have been drilled inside the study

region of Pakistan beneath water complexities, at a depth of two hundred meters. Presently, the Miocene sands, besides the epoch carbonate extent, are considered because of the chief pools (Figure 1b). The northern tip of the Indian plate remained among the chief sedimentary inflows from the Indus, providing evidence of the age of these facies [22]. The foundation chart within the studied zone, displaying the seismic-based data set including the high-resolution seismic profiles (AA′, BB′, and CC′) and the well used in the present study are illustrated in Figure 1c.
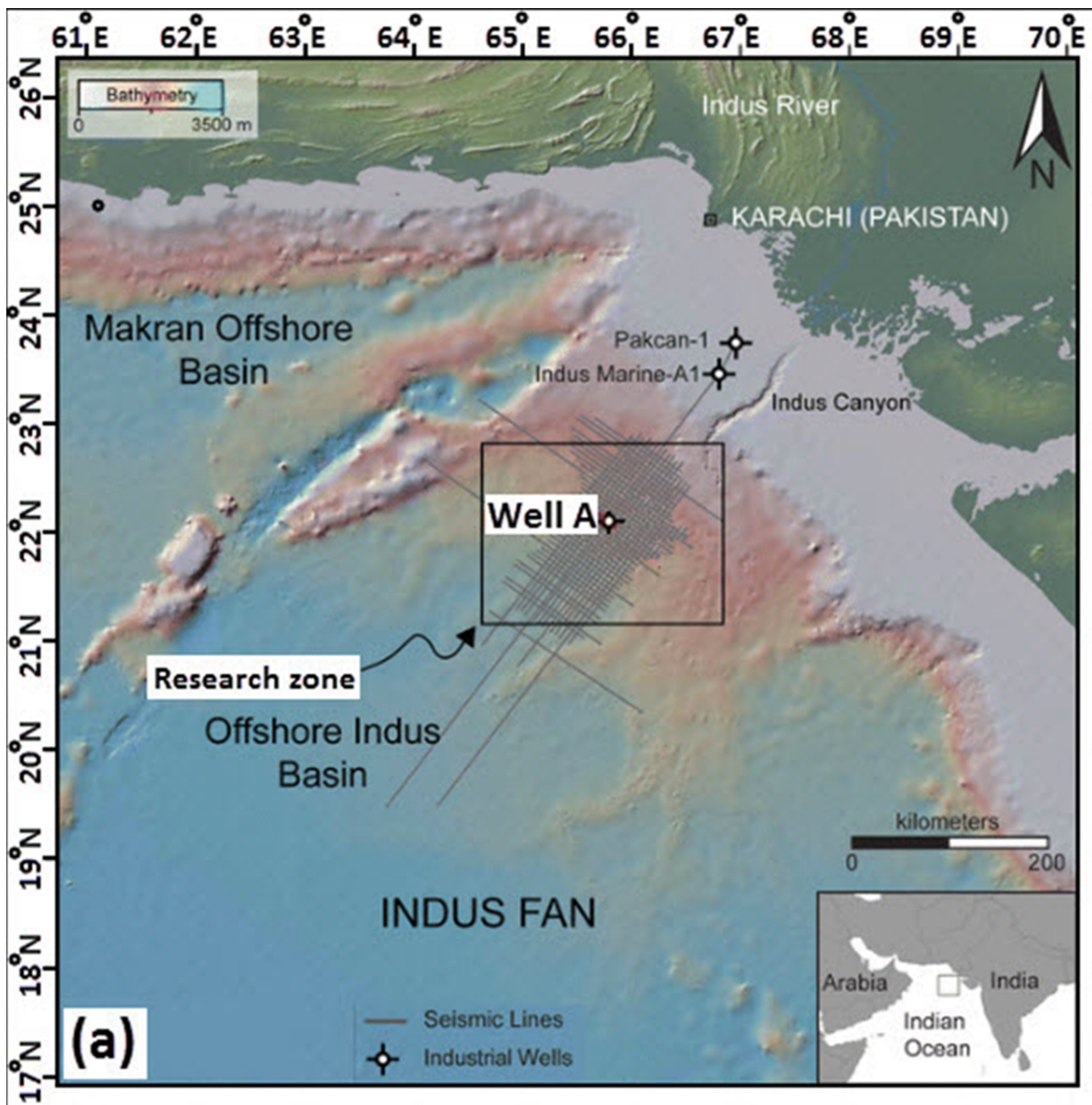
Figure 1. *Cont.*
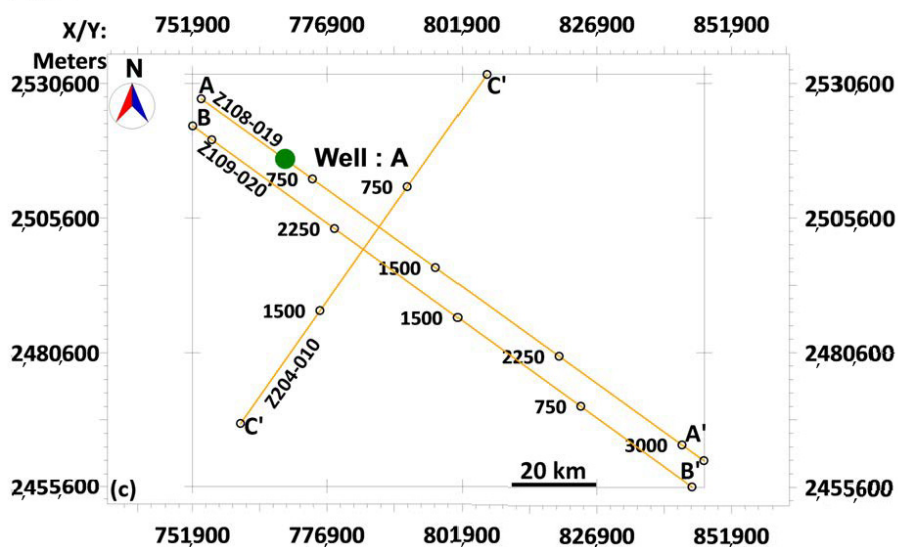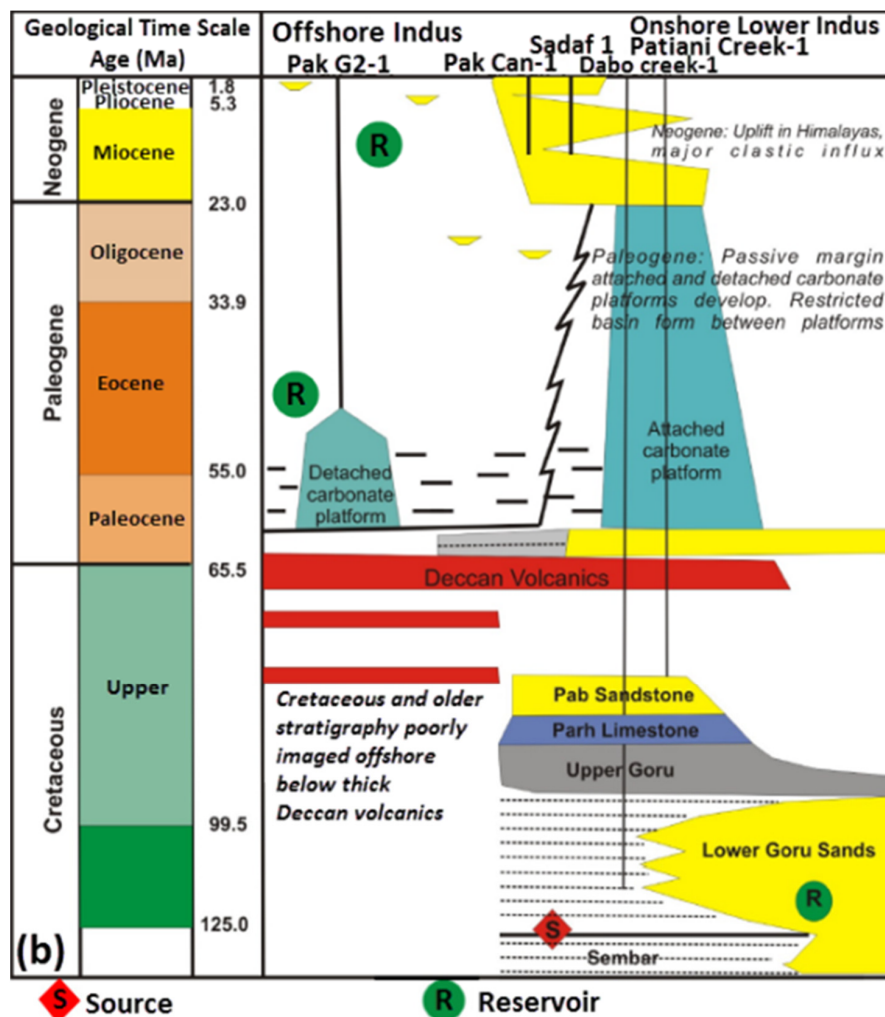
Figure 1. (**a**) Geographical configuration of the offshore Indus Basin (OIB), showing the research area (black box), besides its position, relatively near the Indian deep-sea residues discovered at the cutting-edge of the lowermost right zone (modified after [23]), (**b**) Comprehensive stratigraphic system within the research area, showing the disseminating pools, (**c**) The foundation chart within the studied zone, which shows the seismic-based and wells catalog used in this study.

For deep-water basins, the most probable source breaks are at the cutting-edge of the Miocene, besides Paleocene-Eocene breaks. Reasonable-quality source rocks of the early Miocene age remained contemporary on the shelf, covering a 300-m unit with a normal total organic carbon (TOC) of 2%. Minor quantities of gas were verified under sandstone above this break, emphasizing the occurrence of a thermogenic gas kitchen towards the south underneath the external shelf beside the superior slope. This kitchen might determine the forecast lengthways of the rollover development on the upper slope [22]. Paleocene-to-Eocene carbonates have prospective source shales inside the petroleum system. The focal point of the present study is the portrayal of Miocene sands that fuse the different potential stratigraphically trapped depositional plays among the oil- and gas-bearing channelized-basin floor fans (Figure 2).
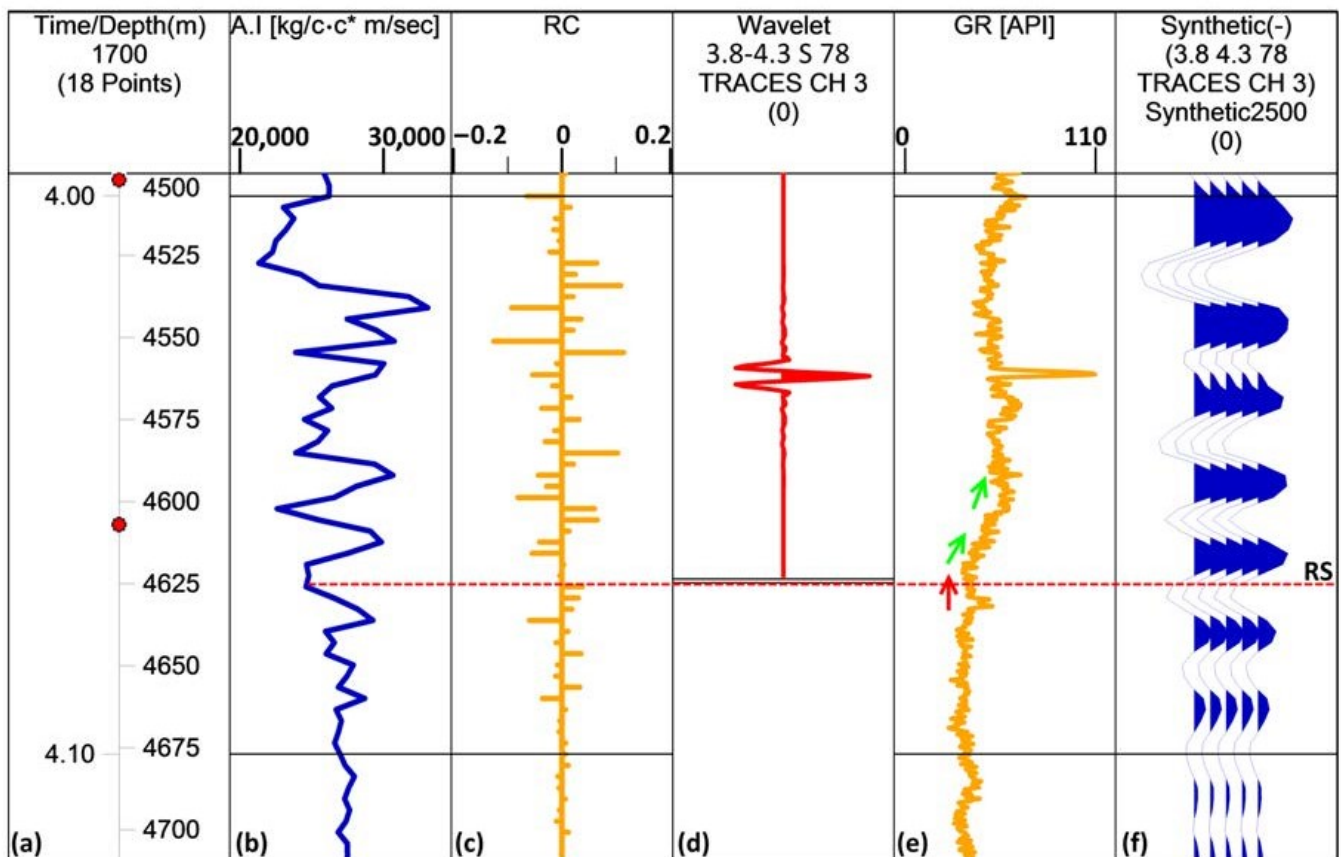

Figure 2. Synthetic seismograms generated at Well A along with panels (**a**) Time-Depth (T/D) s/m, (**b**) Acoustic impedance log generated at Well A, (**c**) reflection coefficients, (**d**) Seismically extracted wavelet inside the research zone (3.6 to 4.2 s), where the basin floor fans are analyzed, (**e**) Gamma-ray log (orange curve) showing the trend of sea-level fall (red arrow) and subsequent rise (green arrows), and (**f**) Seismic-based traces along dip-line A–A′.

The seal might be interpretable in a couple of zones from erosional channels and mud volcanoes (Figure 3a–c). The occurrence of low stand system tracts (LST) can be seen within the research zone, which caused the deposition of basin floor fans throughout a rapidly falling sea with a negligible increase. This phenomenon is confirmed via onlaps (yellow arrows) (Figure 3c). The focus of exploration is the LST, where these stratigraphic deposits were deposited and delineated using post-stack seismic-based attributes and wedge modeling.
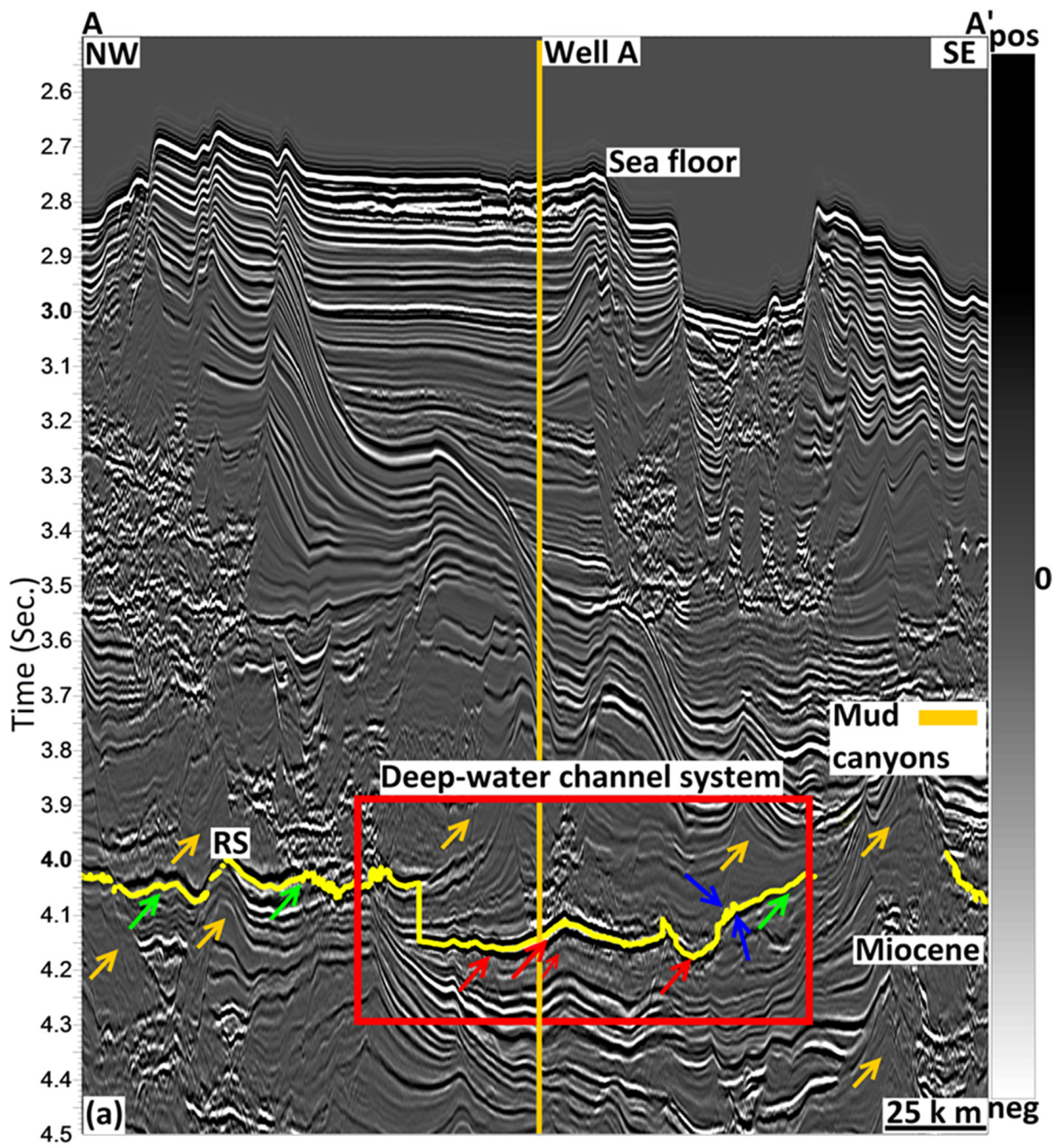
Figure 3. *Cont.*
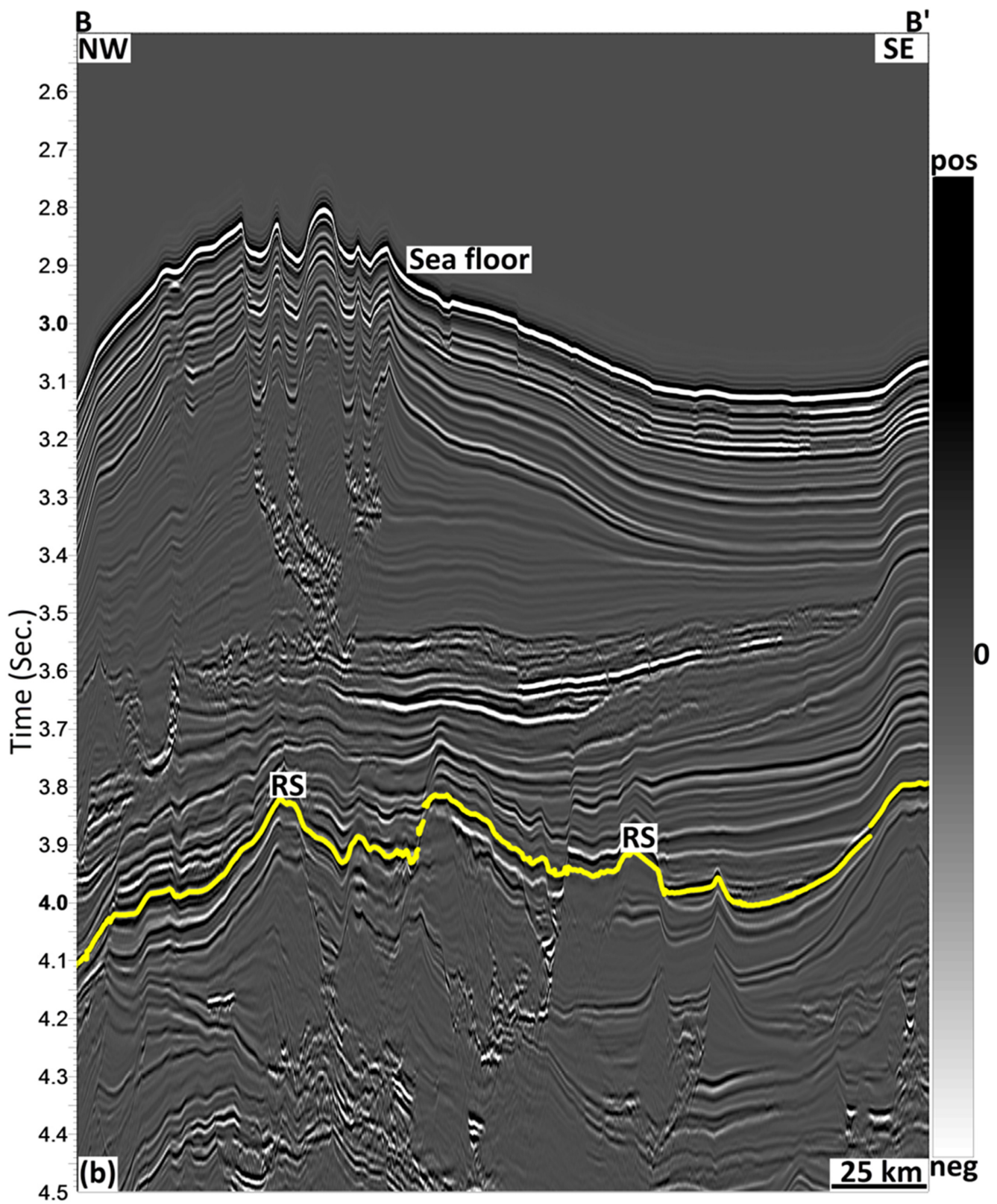
Figure 3. *Cont.*
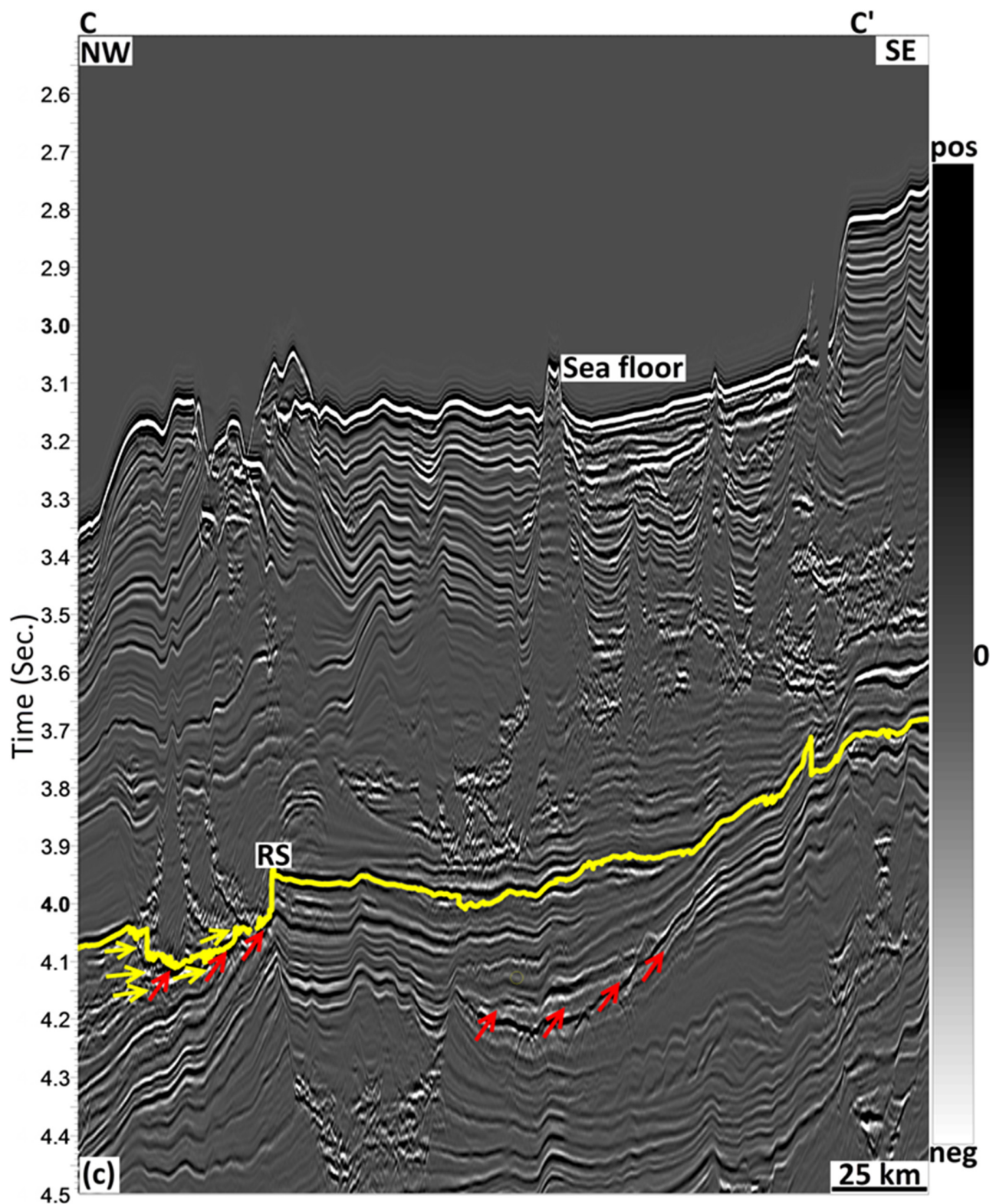
Figure 3. Seismic-based amplitude sections along the deep-water reservoir system (red block) (**a**–**c**) that are analyzed in terms of stratigraphic reservoir characterization of basin floor fans in Figures 4–7, respectively, along A–A′, showing the interpreted reservoir sandstone (RS) within a channelized-basin floor fan, the channel and point bars (red arrows), onlapping (yellow arrows) (**c**), shakeout zone (orange arrows) (**a**), channelized-basin floor fan lens (white arrows) (**a**), erosional zone (blue arrows), and levees (green arrows) (**a**).

3. Materials and Methods

3.1. Database

In Pakistan's Sukkur district, south of the OIB, the Arabian Sea is present. Three high-resolution profiles are included in the seismic-based data set (Figure 1c), including the dip-strike lines (Table 1). The current survey contains a total area of 8970 km^2 inside the study zone. This survey is aimed at exploration, besides portraying the channel-levee system and basin floor fan systems. The data were composed on an illustration interval of 4000 micros by excellence treatment (Table 2). The amplitude is preserved, and the quality is excellent (Table 3). As a result, the clear analytical conclusion provides trustworthy evidence. The velocity fluctuated between 4362 m/s and 3161 m/s, with an interim value of 1700 m/s, also used for the development of synthetic seismograms (Figure 2). Once the seismic-based features and their interpretation have been processed, this velocity is used to determine the overall thickness of reservoir sandstone (Table 4). Between 15 and 6 m are the highest and lowest limits of seismic-based resolution. 12 m is the average tuning thickness.

Table 1. Seismically summaries performed aimed at a valuation of channel-levee pools.

S. No	Seismic Profile	Orientation/Nature	Length (km)
1.	Z108-019 (A–A′)	SW-NE Striking	79
2.	Z109-020 (B–B′)	NW-SE Dipping	115
3.	Z204-010 (C–C′)	NW-SE Dipping	114

Table 2. Comprehensive seismic-based acquirement constraints of the OIB, SW Pakistan.

S. No	Total Exploration Pakistan Indus Offshore Blocks G and H
1.	Recorded By Fugro Geoteam November–December 2000
2.	Reel: 10sfmig2 Dataset: Final Filtered and Scaled Migration
3.	Vessel: R/V Geo Baltic; Shooting Direction 127 Degrees
4.	Data Traces/Record: 480; Auxiliary Traces/Record: 0 Cdp Fold: 80
5.	Sample Int: 2 Ms; Samples/Trace: 2561
6.	Recording Format: Seg-D 8015; Format This Reel: Seg-Y
7.	Recording Filter: 4 Hz (18 Db/Oct)–206 Hz (266 Db/Oct)
8.	Source: Airgun Array; Sp Interval: 37.5 M
9.	Near Offset: 143 M; Cable Length: 6000 M; Group Int: 12.5 M
10.	Traces Sorted by Cdp

Table 3. Comprehensive seismic-based processing constraints of the OIB, SW Pakistan.

S. No	Physical Parameterization
1.	Veritas Dgc Ltd., December 2000–June 2001
2.	Reformat From Seg-D and Edit
3.	Dephase And Anti-Alias Filter, Resample to 4 Ms
4.	6 Hz 18 dB/Oct Low Cut Filter; 2 d Navigation Assignment
5.	Back Out Dephase Filter; Reapply Zero Phasing Filter With Receiver Ghost
6.	Spherical Divergence Correction—T in Water Layer V Squared T In Data
7.	Create 240-Fold Supergather; Nmo Correct with Multiple Velocity Function
8.	500 ms Agc; Radon Demultiple—Transform −1800 To + 300 Notch −200 To + 30

Table 3. *Cont.*

S. No	Physical Parameterization
9.	Applied from 1.8 Times the Water Bottom; 500 ms Agc Removed
10.	Every Other Cdp Dropped to Give 12.5 m Cdp Spacing
11.	500 ms Agc; Radon Demultiple—Transform −1800 To + 300 Notch −200 To + 300
12.	500 ms Agc Removed; Multiple Velocity Nmo Removed
13.	Nmo Correct with Initial Picked Velocities
14.	Stretch Mute; 6hz Low Cut Filter
15.	2 ddmo—Fk Algorithm
16.	Pre-Stack Time Migration Using a Single Minimum Vz Velocity Function
17.	Initial Picked Nmo Removed
18.	Nmo Correction with Picked Post Pstm Velocities Inner and Outer Trace Mute
19.	2 d Stack Conventional Stack to 1 Sec Below Reef Time Weighted Median Stack
20.	Diffract Using a Single Minimum Vz Velocity Function
21.	2 d Omega-X Migration Using 97.5% Smoothed Velocities
22.	Time Variant Filtering 2 Second Balance Gates Overlapped By 50%
23.	Sp 101 at Cdp 480, 6 Cdps per Shot Shotpoints Annotated at Cdp Position

Table 4. Computation of petrophysical attributes within sand-filled channel.

S. No	Seismic Attributes	Reservoir	Velocity [V] [m/s]	Time Window [T] [s]	Thickness [m] = V × T
1.	Seismic amplitude	Channelized-BFF	1700	4.157–4.166 = 0.009	15
2.	Instantaneous frequency	Channelized-BFF	1700	4.153–4.165 = 0.012	21
3.	Envelope strength	Channelized-BFF	1700	4.149–4.171 = 0.022	38
4.	Sweetness	Channelized-BFF	1700	4.150–4.168 = 0.018	33

The current survey contains a total area of 8970 km^2 inside the study zone. This survey is aimed at exploration, besides portraying the channel-levee system and basin floor fan systems. The data were composed on an illustration interval of 4000 micros by excellence treatment (Table 2).

3.2. Computations of Seismic-Based Attributes and Their Applications in Stratigraphic Reservoir Characterization

To obtain strong geographical proof after seismic-based statistics aimed at refining the geophysical parameters, a combined seismic-based follow-up analysis was required. Complex seismic-based follow-up is occasionally used to assess seismic characteristics [17]. The seismic features include topographical information such as tremor investigation flagging [24], immediate seismic-based pile evidence characteristics [25], and thinly-distributed strata inside exploration zones [26]. Several aspects of the portrayal of the repository were determined using a variety of seismic-based attributes that were grounded in reality [27].

The fitness of amplitude-derived qualities for the stratigraphic supply portrayal of clastic in addition to carbonate supplies has been confirmed [16,19,20]. In the current analyses, three well-known post-stack seismic-based properties are taken into consideration as a framework for inferring lithological fluctuations, thickness, and porosity angles inside the profound water-filled channel-levee system, as well as the basin floor fans. These properties include seismic-based instant frequency, envelope strength, sweetness, and instant phase (Figures 3–5).

3.3. Instant Phase

The instant phase characteristic is derived through Equation (1):

$$\Phi\ (t) = \arctan\ (H\ (t)/T\ (t)) \tag{1}$$

where the seismic-based trace T (t) and the situation Hilbert transform H (t) are connected to the envelope E (t) by the phase Φ (t) through Equations (2) and (3):

$$T\ (t) = E\ (t)\ \cos\ (\Phi\ (t)) \tag{2}$$

$$H\ (t) = E\ (t)\ \sin\ (\Phi\ (t)) \tag{3}$$

Instant phase remains restrained at cutting-edge degrees $(-\pi, \pi)$. It is independent of amplitude-based attributes and exhibits continuousness and measure cutoff. It displays a sheet that is glowing [18]. Lateral phase prospect must not alter the cutting-edge standard; variations in container ascent here remain a preference problem, or else there is uncertainty about the coating variants crosswise owing to "sink-holes" or additional factors.

The finest pointer of adjacent continuousness also indicates the phase constituent of the wave propagation. Its container is not counted toward calculating the phase speed, consuming no amplitude evidence, and henceforth, the entire mechanical pattern container remains understood [18]. It is useful for demonstrating endurance, order limitations, comprehensive imagining of bedding outlines, and cutting-edge calculation of instant occurrence, besides quickening. Particularly once the practical cutting-edge combination is achieved by the instant frequency, it can be performed by way of a DHI [16] in terms of applied cutting-edge current event learning aimed at relating the impenetrable and absorbent channelized-basin floor fans through the phase reverse (Figure 5e).

3.4. Computation of Instant Frequency

Instant frequency characterizes the mean amplitude of the wavelet. Instant frequency (F (t)) stays the time imitative of the phase, i.e., the degree (dt) of variation of the phase (Φ (t)), is also assumed via Equation (4):

$$F\ (t) = d\ (\Phi\ (t))/dt \tag{4}$$

The immediate frequency can be used to indicate bedding breadth in addition to lithological constraints. That is consistent with the seismic-based wavelet's normal frequency (centroid) of the amplitude band. The limits of truncated impedance thin beds are indicated by seismic-based charisma relations. For instance, using low-frequency variance sideways and phase reversal, it can function as a direct hydrocarbon indicator (DHI) [19]. The unconsolidated sandstone occasionally protrudes towards the oil and gas content of the holes, emphasizing this effect. Lower frequency region pointers, muddled image region pointers, and bed thickness pointers are all equally affected by breakage region pointers. Lower frequencies designate sandstone-rich bedding in addition to sand-shale points, while higher frequencies denote sharp borders or thin shales. According to the readings currently available, this tool is directed at the exploratory demarcation of parallels alongside the nearby thick sandstone beds secreting the basin floor fans (Figures 4b and 5b).
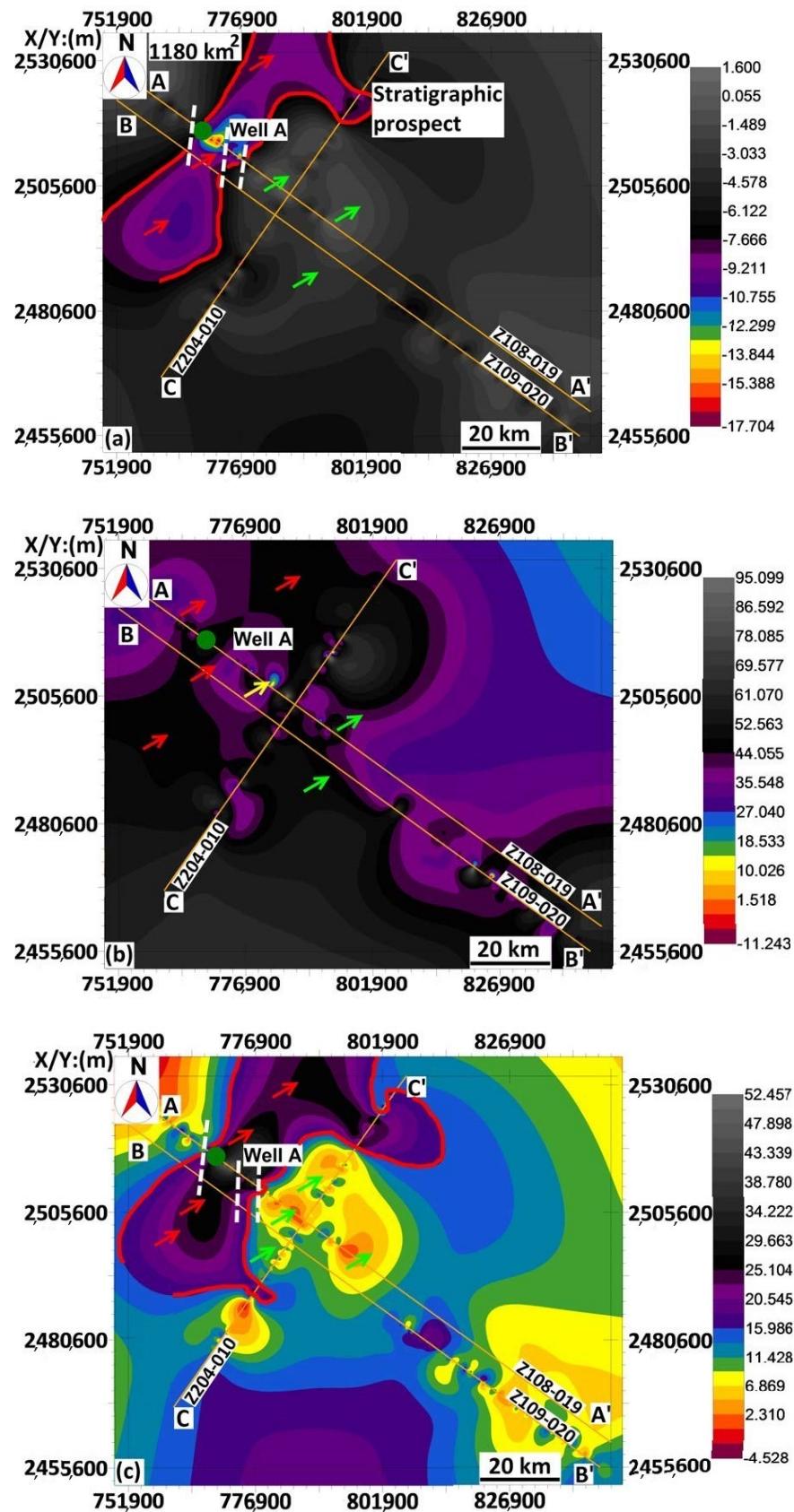
Figure 4. Plots of amplitude-based magnitudes of seismic-based attributes, (**a**) Seismic-based amplitude, (**b**) Instant frequency. (**c**) Trace envelope, showing the distribution of reservoir sands (channelized-basin floor fans) (red arrows) and non-reservoir shales (green arrows).

3.5. Computation of Envelope Strength

To characterize the hydrocarbon reservoir, the envelope strength is an effective tool based on a physical attribute, including the presentation of the AI distinction and therefore the influence of a seismic-based event (Figures 4c and 5c) [18].

The envelope strength (E) is designed after the composite trace-based attribute, as shown by Equation (5):

$$E(t) = \sqrt{T^2(t) + H^2(t)} \tag{5}$$

where T (t) is the seismic trace, H (t) is Hilbert's transform of T (t), and H (t) is a 900-phase shift of T (t).

The envelope strength stands for the envelope of the amplitude of seismic-based traces. It requires a low-frequency advent besides solitary progressive magnitudes. It regularly highlights the chief seismic-based landscapes. The envelope characterizes the instantaneous strength of the signal and how it compares to the reflectivity constants in terms of its degree [18].

It has various applications in stratigraphic reservoir characterization, which include the identification of "sweet spots" related to gas accumulation, the delineation of seismic-based stratigraphic surfaces, the elaboration of tuning effects due to intercalations of sand-shale and carbonates-shale groups and their accumulation within the heterogeneous reservoirs, the chief fluctuations in depositional backgrounds, the reconnaissance delineation of porous and productive lithology, and as a sand-shale discriminator [16,17]. This tool designates the group rather than the phase component of the seismic-based wave propagation. Therefore, the tuning effect due to shale distribution within the clastic and carbonate reservoirs can be distinguished, which can cause ambiguity in the prediction of porous sandstone. High values are inferred from the porous sandstone or carbonate reservoirs. On the contrary, the low values are interpreted as the massive shale distribution [18] (Figures 4c and 5c).
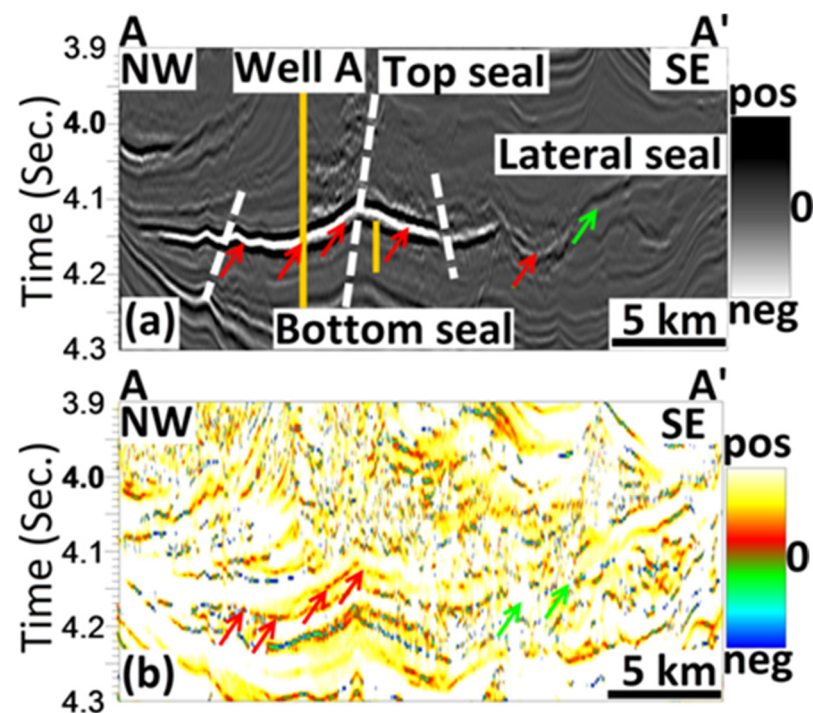

Figure 5. *Cont.*
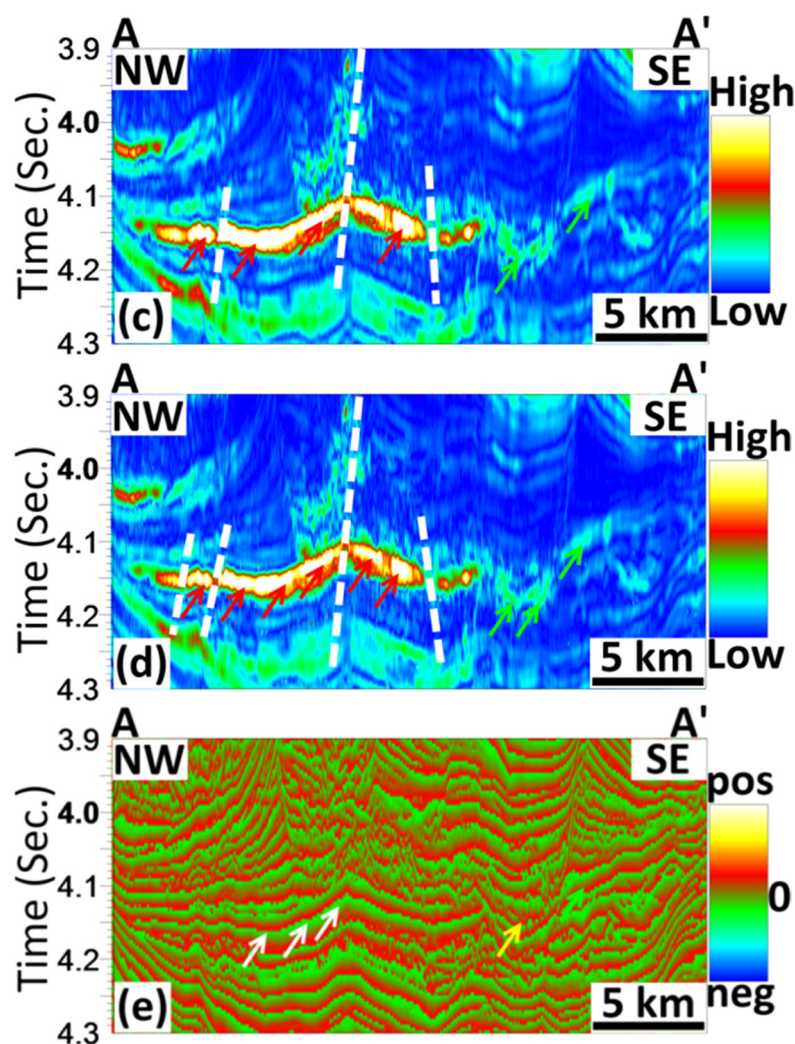
Figure 5. Processing of seismic-based attributes magnitudes along the deep-marine channel system (**a**) Seismic-based amplitude, (**b**) Instant frequency, (**c**) Envelope amplitude, (**d**) Sweetness, and (**e**). Instant phase, showing the distribution of sandstone inside channel sandstone, point bars (red arrows), and shale-filled levees (green arrows) along with the marked fault system (white-dashed lines). Sweetness, being a hybrid attribute, provides better illumination of potential lithologies, faults, and true thickness of the channelized-basin floor fans compared to the other conventional seismic-based attributes.

3.6. Sweetness Computation

Equation (6) shows the computation of sweetness magnitude, which was derived by dividing the reflection strength (or envelope strength) by the square root of instant frequency [28].

$$\text{Sweetness} = \text{envelope strength}/[\text{square root (instant frequency)}] \qquad (6)$$

High values are established for porous and thick clastic facies, while lower magnitudes are inferred from the non-porous and seal facies (Figure 5d).

4. Results and Discussion

4.1. Seismic-Based Amplitude Standardization and Sedimentary Characteristics of Deep-Water Basin Floor Fans

The development of synthetic seismograms is a valid criterion for achieving accurate subsurface seismic-based data interpretations [16]. The purpose of this forward model is to

delineate the exact location marking the reservoir and the non-reservoir (seal or cap) zone with less risk than is usually involved in oil and gas exploitation. This approach can lead to the successful exploitation of oil and gas reservoirs. Therefore, a forward model is developed to achieve seismic-based data interpretation standards (SDIS) by convolving the reflectivity series with the extracted wavelet (Figure 2). This model also shows that the sandstone was deposited during sea-level fall inside the low-stand system (LST) (red arrows) that is sealed by the transgressive clastics (green arrows) that form economically viable oil and gas shows (Figure 2). The acoustic impedance (AI) of sandstone is low compared to that of shales. Therefore, the reservoir sandstone (RS) strait is interpreted based on this model, as marked on the trough throughout the seismic-based profile, i.e., A–A′, B–B′, and C–C′ (Figure 3a–c). The channel-levee system is best exposed on A–A′, as compared to B–B′ and C–C′, respectively (Figure 3). The channel-levee system (red and green arrows) is seen throughout the A–A′ profile (Figure 3). The basin floor fans have a time window of 3.6 to 4.2 s (Figure 3). The whole study is focused on the lenticular sandstone lens (LSL), which remained detectable along the marked RS formation (Figures 4–7). The onlapping (yellow arrows) is seen on the A–A′, which provides solid evidence of a rapidly falling sea and subsequent substantial coarser grains of sedimentary facies. Moreover, the reflection continuity is uniform, which validates the presence of porous pools inside the deep-water settings (red block).

A submarine fan (SF) is generally associated with the erosion of canyons into slopes and shelves. The mud-filled high amplitude canyons (orange arrows) erode the sediments that are subsequently filled inside the deep-water pools. The thickness of shale that serves as the top seal is 930 m, the lateral mud-filled canyons are 1190 m, and the thick bottom seal is ~10 m, which hence provides evidence for the presence of a vibrant petroleum play. Since the seismic-based amplitude is classified as a broadband attribute, that has shown some tuning effects for quantitative stratigraphic analyses [19]. Moreover, the basin deposits are more pronounced as compared to the channel-levee system. Therefore, the seismic-based attribute processing is focused on characterizing the stratigraphy of sand-filled basin floor fans to delineate their accurate lateral and vertical distribution (Figures 4–6).
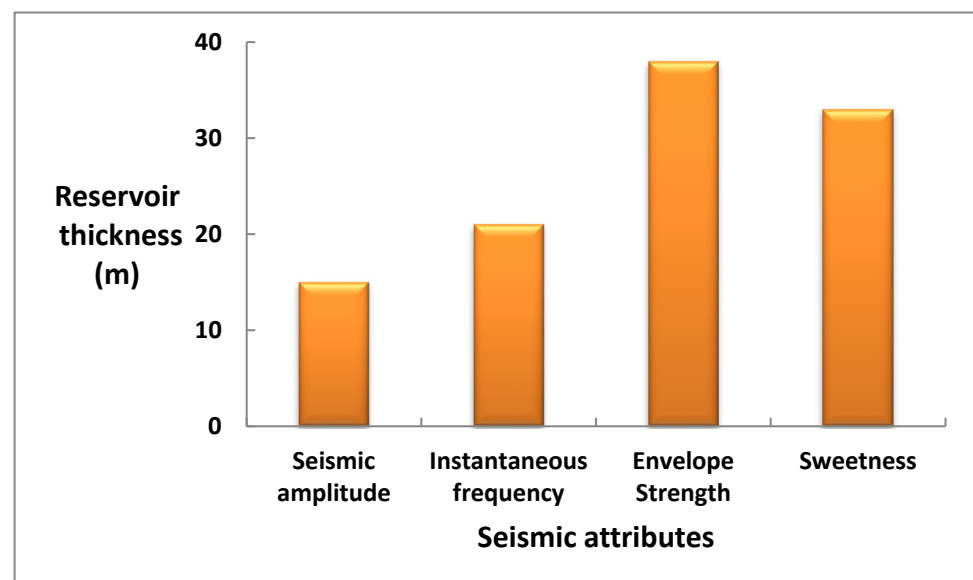

Figure 6. Response of seismic-based attributes against the thickness of reservoir sandstone channelized-basin floor fans. Envelope strength shows higher thickness of basin floor fans as compared to the sweetness. However, the hybrid characteristic of sweetness magnitudes provides a true thickness prediction and accuracy in the characterization of basin floor fans.

4.2. Detection and Characterization of Deep-Water Stratigraphic Prospects

It is important to make a distinction between channelized and non-channelized amplitudes to avoid a false interpretation of seismic-based amplitudes. The non-channelized sub-marine fans, or basin floor fans, are developed on the distal side of a channel-levee system. Generally, the flow is detached from the basin floor, which results in poor geomorphology and lower energy magnitude as it moves from the proximal to the middle and lower segments, where the channels are less likely to appear and hence are less favorable for hydrocarbon exploitation [29]. However, the channelized basin floor fans that are developed on the proximal side of a channel-levee system inside the basin show excellent reservoir connectivity and flow, resulting in the development of excellent geomorphological features. Moreover, they experience high N/G, porosity, thickness, and higher energy assembly due to their association with river delta systems, and hence they serve as fruitful locations for the successful exploitation of stratigraphic pools. These potential stratigraphic traps decrease gradually in sandstone content, with 90% sandstone in the proximal areas [29,30]. These observations can be assessed on the seismic section (Figure 3a) and the horizontal attribute-based mapping (Figure 4). An excellent imaging of the channel-levee system is seen, and hence, these basin floor fans are interpreted as channelized basin floor fans. Figure 4a–c shows the delineation of laterally disseminated basin floor fans by seismic-based amplitude, instantaneous frequency, and envelope strength, respectively.

An NNE-SW-oriented channelized-basin floor fan geomorphic feature (red boundary) is seen on the seismic-based amplitude. This stratigraphic prospect has an area of 1180 km^2. The least bright negative amplitudes (red arrows with the least AI) near Well A are interpreted as channel sandstone. This basin floor fans reservoir bed shale-outs (higher AI) in the eastern margins (green arrows) and hence validates the SDIS (Figure 2). The instant frequency shows the thick sandstone (red arrows) exactly as it is delineated by the seismic-based amplitude attribute. The envelope strength facilitates true thick reservoir distribution and images of the true geomorphology of basin floor fans (red boundary). The vertical slices of seismic-based attributes correlate with the vertical distribution and provide physical characterization (lithology prediction, thickness, and porousness) of basin floor fan stratigraphy (Figure 5).

4.3. Seismic-Based Attributes Analyses for Quantitative Reservoir Stratigraphy and Lithological and Thickness Analysis

Figure 5a–e shows the processing of seismic-based attributes for the channelized-basin floor fans. The SDIS validates the trough amplitudes as the sandstone body, and hence, the basin floor fan is a sand-filled reservoir. A lenticular sandstone lens (LSL) (red arrows), point bars (red arrows), levees (green arrows), and faults (white dashed lines) are seen in the seismic-based amplitude slice (Figure 5a). These faults are interpreted as the perpendicular normal system [31], which provides vertical migration paths for reservoir facies that are trapped in the LSL. The instantaneous frequency shows the low-frequency anomaly (red arrows) along this LSL, and hence, it is inferred to be the hydrocarbon-bearing LSL [16,18] (Figure 5b).

The envelope strength is a proven tool for the illumination of productive reservoir zones by eliminating the shale effects, and hence, it interprets the true reservoir lithology (red arrows) and the non-reservoir levees (green arrows) (Figure 5c). Sweetness has proven its applicability in the accurate demarcation of stratigraphic prospecting pools [16,19]. The sweetness slice shows high-magnitude waves inside the reservoir LSL (red arrows) that shake out (green arrows) into the NE parts of the reservoir (Figure 5d). Moreover, the faults are far better illustrated by sweetness as compared to previous attributes having three faults. The instant phase also confirms the presence of a stratigraphic prospect (red arrows), where a strong phase reversal (white arrows) is observed along the LSL. The thickness analyses can also be seen in the bar graph (Figure 6), which confirms the sweetness's accuracy in the prediction of thickness by the combination of instant frequency and envelope strength. The seismic-based amplitude shows a 15-m thickness for this LSL (Table 4). The instant frequency shows 21 m of thickness, the envelope strength shows

38 m of thickness, and sweetness shows 33 m of thickness, with a lateral distribution of 15 km that is observed along this LSL. Since sweetness is the combination of envelope strength and instant frequency (Equation (6)), it is a hybrid attribute. Therefore, it predicts the true thickness, whereas the envelope strength shows some tuning effects. And the shale effects were not able to be eliminated only via the tool, i.e., envelope strength. The wedge model for the identified LSL is developed to corroborate the accuracy of sweetness application in forecasting true lithology and thickness, and hence, porous hydrocarbon resources (Figure 7).
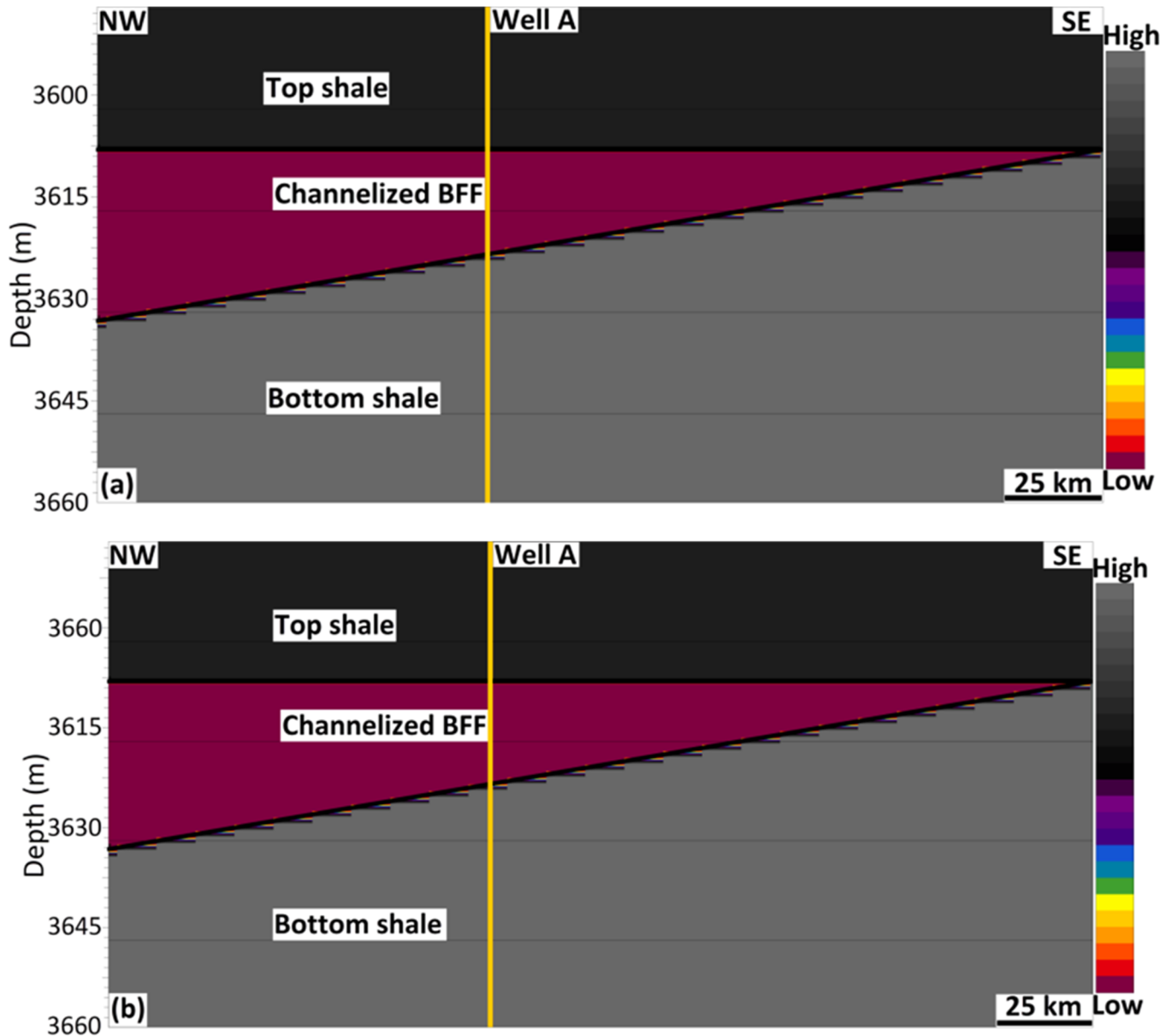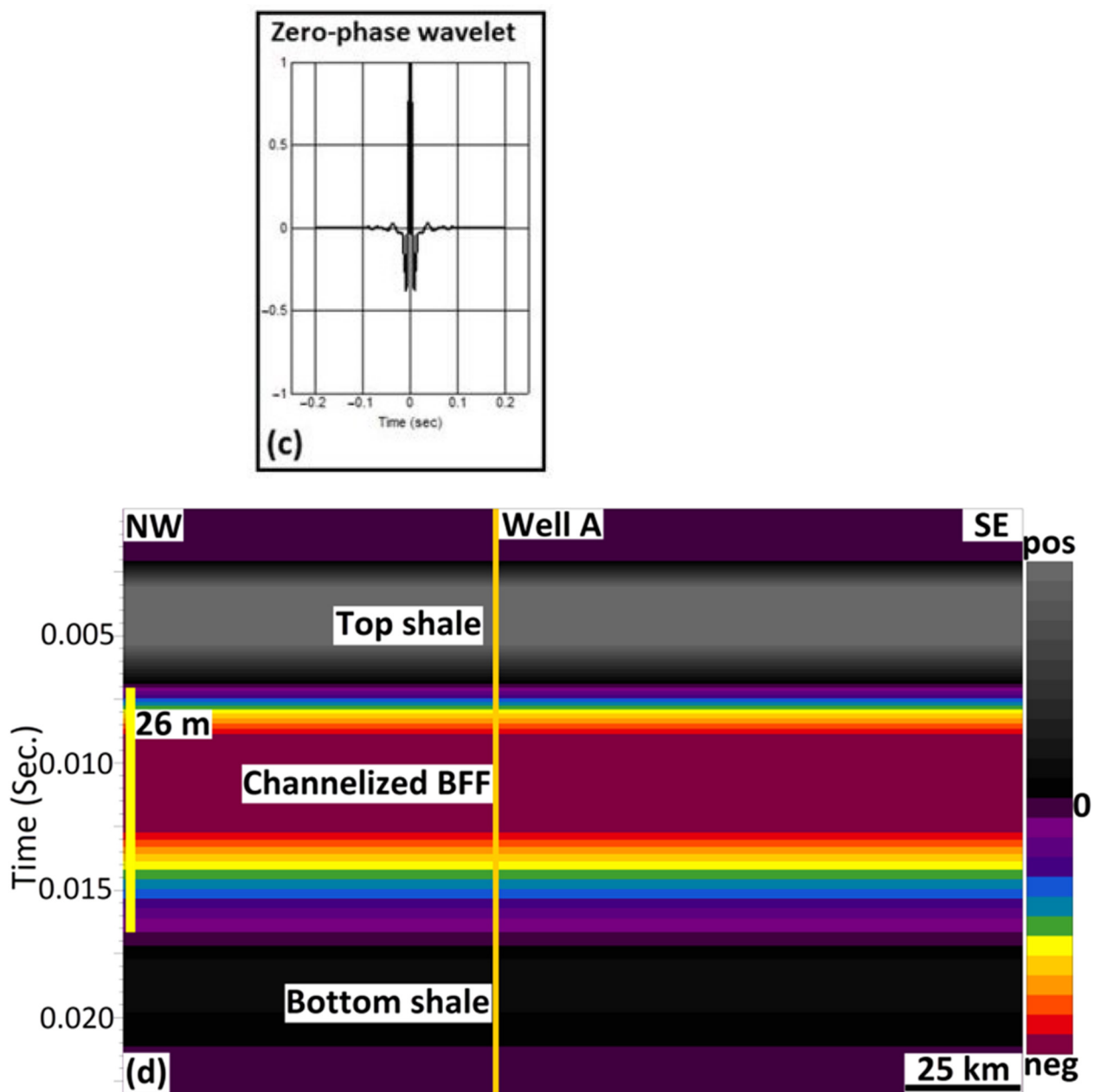

Figure 7. *Cont.*

Figure 7. Schematic steps applied for developing deep-water channelized-basin floor fans stratigraphic system (**a**) Original density prototypical, (**b**) Original velocity prototypical, (**c**) Zero-phase seismic-based wavelet withdrawal at Well A, and (**d**) Resultant acoustic impedance profile developed after convolution of initial models (**a**) and (**b**) with zero-phase wavelet (**c**). The total thickness of sand-filled channelized-basin floor fans is 26 m, which is embedded from the top and bottom by massive shales and developing a vibrant stratigraphic play.

4.4. Static Wedge Modeling and Implications for Oil and Gas Exploitation and Implications of Basin Floor Fans

Static wedge modeling is a robust tool for discrimination of reservoirs (clastic and carbonate) and non-reservoirs (seal and cap), and hence, a proven direct hydrocarbon indicator (DHI) [16,19,32]. Figure 7a,b show the initial density and velocity models (IDM and IVM). These IDM and IVM are collectively convolved with the seismically extracted zero-phase wavelet (Figure 7c), and that resulted in an excellent reflection-based impedance model for channelized basin floor fans (Figure 7d). This wedge model shows the lowest impedance LSL that is embedded in the top and bottom seals and confirms the future hydrocarbon-bearing

prospect. The thickness of LSL is 26 m with a lateral distribution of ~64 km, while the thickness predicted by sweetness is 33 m. Therefore, this wedge model provides ~75% correlation of the thickness of the LSL, as measured by sweetness magnitudes.

The practical implication of stratigraphic explorations in that basin is the proven oil and gas plays [1,3,5]. These implications are accurately resolved by the sweetness (Figures 5d and 6) and wedge modeling tools (Figure 7). Therefore, the wedge model, together with the sweetness magnitudes, provide solid validations for a stratigraphic play.

5. Comparative Analysis of Geophysical Tools

Our results provide the transparency that the deep-water depositional systems can be characterized using seismic-based attributes and seismic-based forward modeling techniques within the OIB, in SW Pakistan. The processing of post-stack seismic-based attributes was a better approach for analyzing the lithology and thicknesses of reservoirs and, hence, provided additional information without logging the data.

Various geophysical and geological techniques have been industrialized and are aimed at the characterization of stratigraphic plays, i.e., geochemical section analyses, seismic-based inversion, and so on. We used seismic-based attributes to unravel the reflectivity response in terms of seismic-based statistical inferences aimed at deep-water clastics. Compound attribute-based analytical approaches, such as those provided via quantitative-based visualization, complement the robust amplitude lengthwise of the basin floor fan bed event, which has established its applicability towards recognizing upcoming predictions. The consequences of the immediate features elect that those seismic-based features examined can remain performed aimed at the description of assembly and stratigraphy [13,33–35]. Preceding interpretations display approximately the same class of structural and petrophysical examination [22]. However, to place the suite of exploration, production, and development wells, there is a multitude of essential steps towards reassessing the OIB in terms of stratigraphy using advanced seismic-based technology such as the one applied in the present case study. The conventional seismic-based attributes, such as seismic-based amplitude, instant frequency, and envelope strength, predict the true lithology and some traces of faults (Figure 5a–c). However, the sweetness magnitude is the proven tool for achieving complete reservoir characterization goals, i.e., predicting the accurate lithology, thickness, discrimination of reservoir fluids, detection of faults, and hence, the complete petroleum system's elements [16]. Therefore, we predicted the true lithologies (shale and sandstone), faults, and accurate thickness (Figure 5d) (Table 3). Moreover, wedge modeling has proven its validity in the delineation of conventional and unconventional (clastics and carbonates) stratigraphic plays inside the Indus Basin of Pakistan [16,19,20]. Moreover, when the zero-phased wavelet is extracted from the same seismic-based line passing through the well, it can provide accuracy in the delineation of thin bedding. This will image the real-time sedimentary sequences with real-time traces, which were removed and convolved with the density and velocity modeling to invert the internal stratigraphy (Figure 7). This is because the conventional synthetic seismogram may skip the real-time traces of the reservoir because of the unavailability of the vertical seismic-based profile (VSP), or check shot survey in the public domain. The band-limited seismic-based amplitude is never a consistent device aimed at predicting and characterizing these stratigraphic reservoirs. Additionally, this approach will provide better seismic-to-well tie ads compared to the conventional synthetic forward modeling as performed in Figure 2. Therefore, in the present case study, it is evident that this wedge modeling tool as per routine proved that the channelized-basin floor sandstones are bounded by top and bottom by massive shales and hence develop into a vital stratigraphic play (Figure 7). Moreover, the thickness predicted by the wedge model is 26 m, which is very close to the sweetness magnitude, i.e., 33 m. Therefore, the 75% correlation of thickness prediction by these two tools (Figures 5d and 7). Therefore, the sweetness attribute can be used as an independent true lithology and thickness prediction in amplitude-based seismic-based attribute classification. Hence, it provides solid proof for the exploitation of channelized-basin floor fans' stratigraphic plays for future field development that are yet to be stratigraphically explored.

Future Stratigraphic Implications

Converging towards an event per Deng et al. [17], reflection strength aimed at the identification of lithology; nonetheless, this tool failed in the present study (Figure 5c) and was found to be limited in accurately obtaining the true thickness of the channelized basin floor fans. However, being a hybrid attribute, sweetness provides better thickness prediction and discriminates the true composition of sandstone and shale, which usually occurs due to the tuning effects of band-limited seismic-based amplitude data (Figure 5a–c) and cannot be detected using the band-limited seismic-based amplitude data [16] (Figure 5d). The purpose of incorporating Figure 7 is just to provide evidence that, as we know, providing some pieces of evidence makes the explorations a logical progression. Therefore, to compare the results of real-time processing of seismic-based attributes with wedge modeling is to confirm that the lithology is bounded by top and bottom shale, which are two vital aspects for basin floor fans to become vibrant stratigraphic plays; also, to contrast the thickness as determined by real-time seismic attribute processing with the wedge modeling prediction of lithology and thickness restrictions. Therefore, these were two objectives that the wedge modeling incorporated. It is evident that the results predicted by sweetness in terms of lithology and thickness are correlated with a 75% correlation, which is good for signatures in a seismic-to-well tie approach as compared to conventional synthetic seismogram generation (Figure 2) and conventional amplitude mapping without being processed via post-stack attributes. Because in conventional synthetic seismogram generation (SDIS), a single trace is obtained after convolving the reflectivity with the wavelet extraction, a well location is determined. But, in the wedge modeling, a complete seismic-based section in the form of inverted reflection-based acoustic impedance is obtained (Figure 7). This inverted section can better explain the internal stratigraphy as compared to a single seismic-to-well tie approach (SDIS) (Figure 2). The wedge modeling also acts as a direct hydrocarbon indicator (DHI) and, hence, should be incorporated into conventional stratigraphic exploration schemes for de-risking the stratigraphic prospects [16]. Moreover, this scheme of stratigraphic exploration can be used as an analog globally in the Karoo Basin, South Africa, where the detailed seismic-based geomorphology of the potential stratigraphic plays within basin floor fans exists in an enormous domain [30].

Therefore, we suggest that the sweetness and wedge modeling tools can be used to achieve the practical implications of the deep-water depositional systems of these stratigraphic plays, i.e., channelized-basin floor fans are compartmentalized inside the highly variable mud-filled lithologies that make excellent stratigraphic traps [1,3,5]. Therefore, there is an urgent need to re-evaluate the zone by designing new 3D ventures. 3D seismic-based data will not only provide a more accurate stratigraphic resolution as compared to the present case study, i.e., 33 m (Figure 5), but has also become helpful in the overall depositional model, and hence, better production can be achieved from this extensively under-explored OIB in terms of stratigraphic plays. Also, the oil and gas groups are interested in the east-west fluctuations of reservoir facies inside the oil and gas basins of Pakistan [16]. Therefore, the presented workflow may be helpful in future strategic decision-making for extracting more hydrocarbons with fewer risks than are usually involved in structurally trapped reservoirs.

6. Conclusions

- This work uses high-resolution seismic-based profiles to describe the channelized-basin floor fan reservoirs in the OIB, SW Pakistan, in terms of lithology, thickness, and perhaps porosity impacts.
- The execution of seismic-based attributes and wedge modeling tools remain developed for resolving and characterization of porous and gas-bearing pools by the high-resolution seismic-based sketches confidential to the OIB, SW Pakistan.
- The seismic-based amplitude and envelope strength slices better delineate the geomorphology of sand-filled channelized-basin floor fans as compared to the instant frequency magnitudes.

- The sweetness magnitudes predict the thickness of channelized-basin floor fans as 33 m, faults, and porous litho-facies that complete a vital petroleum system. However, these porous lithofacies were unable to discriminate between the reservoir and non-reservoir due to loss of tuning effects of bandlimited seismic attributes.

- The solo applications of seismic attributes, such as sweetness, remained limited in deciphering the tuning effects of the shale intercalations into the reservoir formation. That is why the accuracy of this attribute was limited in deciphering the lateral and vertical extents of this basin floor fan facies. Additionally, thin-bedded reservoirs are very sensitive to the thin-bed wedge modelling tools, such as the simulation performed in this research work. However, wedge modelling resolves a hydrocarbon-bearing channelized-basin floor fans LSL of 26 m thickness with a lateral distribution of ~64 km. There were clear indicators of the shale intercalations of ~7 m thickness, which were poorly resolved, in the sweetness attribute mapping. Therefore, static reservoir simulations could be the ultimate choice in delineating the reservoir and non-reservoir facies within these basin floor fans and to discriminate the domain of channelized segments of the basin floor fans, which were very attractive targets for exploration of the primary stratigraphic traps. Additionally, the channelized BFF have been the most attractive targets in the stratigraphic exploration due to the high sinuosity of the meandering channel belts, which are considered as the primary stratigraphic traps; all the domain conditions prevailed for the development of the pure stratigraphic traps, i.e., the resolvable segments of the top and lateral seals, which were accurately predicted by the static reservoir simulations compared to the sweetness and the other remaining bandlimited seismic amplitude-based attributes. Consequently, this research affirms the bright opportunities to exploit the economically-vibrant stratigraphic schemes in the Offshore Basins besides worldwide deep-water structures.

Data Availability Statement: The data used in this work is available on request to the corresponding author.

Conflicts of Interest: The authors declare no conflict of interest.

References

1. Wu, S.; Han, Q.; Ma, Y.; Dong, D.; Lü, F. Petroleum system in deepwater basins of the northern South China Sea. *J. Earth Sci.* **2009**, *20*, 124–135. [CrossRef]
2. Chen, W. Status and challenges of Chinese deepwater oil and gas development. *Pet. Sci.* **2011**, *8*, 477–484. [CrossRef]
3. Zhu, W.; Zhong, K.; Li, Y.; Xu, Q.; Fang, D. Characteristics of hydrocarbon accumulation and exploration potential of the northern South China Sea deepwater basins. *Chin. Sci. Bull.* **2012**, *57*, 3121–3129. [CrossRef]

4. Moforis, L.; Kontakiotis, G.; Janjuhah, H.T.; Zambetakis-Lekkas, A.; Galanakis, D.; Paschos, P.; Kanellopoulos, C.; Sboras, S.; Besiou, E.; Karakitsios, V.; et al. Sedimentary and Diagenetic Controls across the Cretaceous-Paleogene Transition: New Paleoenvironmental Insights of the External Ionian Zone from the Pelagic Carbonates of the Gardiki Section (Epirus, Western Greece). *J. Mar. Sci. Eng.* **2022**, *10*, 1948. [CrossRef]

5. Liu, L.; Zhang, T.; Zhao, X.; Wu, S.; Hu, J.; Wang, X.; Zhang, Y. Sedimentary architecture models of deepwater turbidite channel systems in the Niger Delta continental slope, West Africa. *Pet. Sci.* **2013**, *10*, 139–148. [CrossRef]

6. Krzywanski, J. Heat Transfer Performance in a Superheater of an Industrial CFBC Using Fuzzy Logic-Based Methods. *Entropy* **2019**, *21*, 919. [CrossRef]

7. Skrobek, D.; Krzywanski, J.; Sosnowski, M.; Kulakowska, A.; Zylka, A.; Grabowska, K.; Ciesielska, K.; Nowak, W. Implementation of deep learning methods in prediction of adsorption processes. *Adv. Eng. Softw.* **2022**, *173*, 103190. [CrossRef]

8. Otwinowski, H.; Krzywanski, J.; Urbaniak, D.; Wylecial, T.; Sosnowski, M. Comprehensive Knowledge-Driven AI System for Air Classification Process. *Materials* **2022**, *15*, 45. [CrossRef] [PubMed]

9. Kambalimath, S.; Deka, P.C. A basic review of fuzzy logic applications in hydrology and water resources. *Appl. Water Sci.* **2020**, *10*, 191. [CrossRef]

10. Khan, M.; Abdelmaksoud, A. Unfolding impacts of freaky tectonics on sedimentary sequences along passive margins: Pioneer findings from western Indian continental margin (Offshore Indus Basin). *Mar. Pet. Geol.* **2020**, *119*, 104499. [CrossRef]

11. Shahzad, K.; Betzler, C.; Qayyum, F. Controls on the Paleogene carbonate platform growth under greenhouse climate conditions (Offshore Indus Basin). *Mar. Pet. Geol.* **2019**, *101*, 519–539. [CrossRef]

12. Hampson, D.P.; Schuelke, J.S.; Quirein, J.A. Use of multiattribute transforms to predict log properties from seismic data. *Geophysics* **2001**, *66*, 220–236. [CrossRef]

13. Chopra, S.; Marfurt, K.J. Seismic attributes—A historical perspective. *Geophysics* **2005**, *70*, 3SO–28SO. [CrossRef]

14. Lee, J.; Byun, J.; Kim, B.; Yoo, D.-G. Delineation of gas hydrate reservoirs in the Ulleung Basin using unsupervised multi-attribute clustering without well log data. *J. Nat. Gas Sci. Eng.* **2017**, *46*, 326–337. [CrossRef]

15. Tayyab, M.N.; Asim, S. Application of spectral decomposition for the detection of fluvial sand reservoirs, Indus Basin, SW Pakistan. *Geosci. J.* **2017**, *21*, 595–605. [CrossRef]

16. Naseer, M.T.; Asim, S. Application of instantaneous spectral analysis and acoustic impedance wedge modeling for imaging the thin beds and fluids of fluvial sand systems of Indus Basin, Pakistan. *J. Earth Syst. Sci.* **2018**, *127*, 97. [CrossRef]

17. Deng, W.A.; Kim, T.; Jang, S. Seismic attributes for characterization of a heavy-oil shaly-sand reservoir in the Muglad Basin of South Sudan. *Geosci. J.* **2018**, *22*, 1027–1039. [CrossRef]

18. Taner, M.T.; Koehler, F.; Sheriff, R. Complex seismic trace analysis. *Geophysics* **1979**, *44*, 1041–1063. [CrossRef]

19. Naseer, M.T.; Asim, S. Porosity prediction of lower cretaceous unconventional resource play, south Indus Basin, Pakistan, using the seismic spectral decomposition technique. *Arab. J. Geosci.* **2018**, *11*, 225. [CrossRef]

20. Naseer, M.T.; Asim, S. Characterization of shallow-marine reservoirs of Lower Eocene carbonates, Pakistan: Continuous wavelet transforms-based spectral decomposition. *J. Nat. Gas Sci. Eng.* **2018**, *56*, 629–649. [CrossRef]

21. Chen, Q.; Sidney, S. Seismic attribute technology for reservoir forecasting and monitoring. *Lead. Edge* **1997**, *16*, 445–448. [CrossRef]

22. Carmichael, S.M.; Akhter, S.; Bennett, J.K.; Fatimi, M.A.; Hosein, K.; Jones, R.W.; Longacre, M.B.; Osborne, M.J.; Tozer, R.S.J. Geology and hydrocarbon potential of the offshore Indus Basin, Pakistan. *Pet. Geosci.* **2009**, *15*, 107–116. [CrossRef]

23. Ryan, W.B.F.; Carbotte, S.M.; Coplan, J.O.; O'Hara, S.; Melkonian, A.; Arko, R.; Weissel, R.A.; Ferrini, V.; Goodwillie, A.; Nitsche, F.; et al. Global Multi-Resolution Topography synthesis. *Geochem. Geophys. Geosystems* **2009**, *10*, Q03014. [CrossRef]

24. Schwartz, S.Y.; Rokosky, J.M. Slow slip events and seismic tremor at circum-Pacific subduction zones. *Rev. Geophys.* **2007**, *45*, RG3004. [CrossRef]

25. Prosser, S. Rift-related linked depositional systems and their seismic expression. *Geol. Soc. Lond. Spec. Publ.* **1993**, *71*, 35–66. [CrossRef]

26. Higuchi, Y.; Yanagimoto, Y.; Hoshi, K.; Unou, S.; Akiba, F.; Tonoike, K.; Koda, K. Cenozoic stratigraphy and sedimentation history of the northern Philippine Sea based on multichannel seismic reflection data. *Island Arc* **2007**, *16*, 374–393. [CrossRef]

27. Grezio, A.; Babeyko, A.; Baptista, M.A.; Behrens, J.; Costa, A.; Davies, G.; Geist, E.L.; Glimsdal, S.; González, F.I.; Griffin, J. Probabilistic tsunami hazard analysis: Multiple sources and global applications. *Rev. Geophys.* **2017**, *55*, 1158–1198. [CrossRef]

28. Radovich, B.J.; Oliveros, R.B. 3-D sequence interpretation of seismic instantaneous attributes from the Gorgon Field. *Lead. Edge* **1998**, *17*, 1286–1293. [CrossRef]

29. Zhang, J.-J.; Wu, S.-H.; Fan, T.-E.; Fan, H.-J.; Jiang, L.; Chen, C.; Wu, Q.-Y.; Lin, P. Research on the architecture of submarine-fan lobes in the Niger Delta Basin, offshore West Africa. *J. Palaeogeogr.* **2016**, *5*, 185–204. [CrossRef]

30. Hansen, L.A.S.; Hodgson, D.M.; Pontén, A.; Bell, D.; Flint, S. Quantification of basin-floor fan pinchouts: Examples from the Karoo Basin, South Africa. *Front. Earth Sci.* **2019**, *7*, 12. [CrossRef]

31. Edwards, C.; Spurgeon, S.K.; Patton, R.J. Sliding mode observers for fault detection and isolation. *Automatica* **2000**, *36*, 541–553. [CrossRef]

32. Marzec, P.; Niepsuj, M.; Bała, M.; Pietsch, K. The application of well logging and seismic modeling to assess the degree of gas saturation in Miocene strata (Carpathian Foredeep, Poland). *Acta Geophys.* **2014**, *62*, 83–115. [CrossRef]

33. Kalkomey, C.T. Potential risks when using seismic attributes as predictors of reservoir properties. *Lead. Edge* **1997**, *16*, 247–251. [CrossRef]

34. Raeesi, M.; Moradzadeh, A.; Ardejani, F.D.; Rahimi, M. Classification and identification of hydrocarbon reservoir lithofacies and their heterogeneity using seismic attributes, logs data and artificial neural networks. *J. Pet. Sci. Eng.* **2012**, *82*, 151–165. [CrossRef]
35. Raef, A.; Mattern, F.; Philip, C.; Totten, M. 3D seismic attributes and well-log facies analysis for prospect identification and evaluation: Interpreted palaeoshoreline implications, Weirman Field, Kansas, USA. *J. Pet. Sci. Eng.* **2015**, *133*, 40–51. [CrossRef]